HHS Public Access

Author manuscript

J Biomech. Author manuscript; available in PMC 2018 August 10.

Published in final edited form as:

J Biomech. 2016 October 03; 49(14): 3281–3288. doi:10.1016/j.jbiomech.2016.08.011.

Embryonically Inspired Scaffolds Regulate Tenogenically Differentiating Cells

Joseph E. Marturano[a], **Nathan R. Schiele**[a], **Zachary A. Schiller**[a], **Thomas V. Galassi**[a], **Matteo Stoppato**[a], and **Catherine K. Kuo**[a,b,*]

[a]Tufts University, Department of Biomedical Engineering, 4 Colby St., Medford, MA 02155

[b]University of Rochester, Department of Biomedical Engineering, Department of Orthopaedics, Center for Musculoskeletal Research, 215 Robert B. Goergen Hall, Rochester, NY 14627

Abstract

Tendon injuries heal as scar tissue with significant dysfunction and propensity to re-injure, motivating efforts to develop stem cell-based therapies for tendon regeneration. For these therapies to succeed, effective cues to guide tenogenesis are needed. Our aim is to identify these cues within the embryonic tendon microenvironment. We recently demonstrated embryonic tendon elastic modulus increases during development and is substantially lower than in adult. Here, we examined how these embryonic mechanical properties influence tenogenically differentiating cells, by culturing embryonic tendon progenitor cells (TPCs) within alginate gel scaffolds fabricated with embryonic tendon mechanical properties. We showed that nano- and microscale moduli of RGD-functionalized alginate gels can be tailored to that of embryonic tendons by adjusting polymer concentration and crosslink density. These gels differentially regulated morphology of encapsulated TPCs as a function of initial elastic modulus. Additionally, higher initial elastic moduli elicited higher mRNA levels of scleraxis and collagen type XII but lower levels of collagen type I, whereas late tendon markers tenomodulin and collagen type III were unaffected. Our results demonstrate the potential to engineer scaffolds with embryonic mechanical properties and to use these scaffolds to regulate the behavior of tenogenically differentiating cells.

Keywords

Tendon; Embryonic; Tissue Engineering; Elastic modulus; Alginate gels

*Corresponding author: Catherine K. Kuo, PhD, Department of Biomedical Engineering, University of Rochester, 215 Robert B. Goergen Hall, PO Box 270168, Rochester, NY 14627-0168, Phone: 1.585.275.2312, Catherine.K.Kuo@rochester.edu.

6. Conflict of Interest Statement

The authors have no conflicts of interest to disclose.

1. Introduction

Tendons are highly collagenous tissues that transmit forces from muscle to bone to enable skeletal motion. Unfortunately, tendon injuries are common and their incidence is increasing (AAOS, 2008; Butler et al., 2004; Lantto et al., 2015). There was a nearly 10-fold increase in the incidence of Achilles tendon ruptures between 1979 and 2011 (Lantto et al., 2015), and more than 135,000 annual Achilles, patellar and rotator cuff tendon surgeries in the USA reported in 2004 (Butler et al., 2004). This is problematic, as even with surgical intervention, injured tendons heal as scar tissues that possess aberrant mechanical and biochemical properties, and are associated with long-term pain and compromised function (Lin et al., 2004). These significant drawbacks are motivating efforts to engineer replacement tendon tissues from stem cells seeded in 3-dimensional (3D) scaffolds. Tendon tissue engineering approaches commonly utilize scaffolds fabricated with the unique characteristics of adult tendon, including high collagen type (Col) I content, highly aligned fibers, and high elastic modulus and tensile strength (Chainani et al., 2013; Chokalingam et al., 2009; Kuo et al., 2010; Kuo and Tuan, 2008; Nirmalanandhan et al., 2008; Qiu et al., 2014; Subramony et al., 2013; Xie et al., 2010; Zhang et al., 2012). However, engineered tissues with normal tendon structure and mechanical properties have not been achieved. One possibility is that tissue engineering strategies based on adult tendon properties are presenting cells with the cues that promote aberrant and dysfunctional tissue formation during healing.

We recently demonstrated that, in contrast to adult tendon, embryonic tendon possesses high cell density, low collagen content, less organized matrix, and low elastic modulus (Marturano et al., 2013; Schiele et al., 2013; Schiele et al., 2015). These findings suggest *embryonic tendon progenitor cells* (TPCs) experience a significantly different microenvironment in embryonic tendon than mature tenocytes do in adult tendon. However, examining the effects of tissue mechanical properties on TPC function during embryonic development is challenged by a multitude of confounding physical and biochemical cues *in vivo*. This study aimed to develop 3D scaffolds with embryonic tendon mechanical properties, and to examine TPC behavior in these microenvironments. Previous studies have shown that TPCs harvested from embryonic tendons are an excellent model system to study stem cell tenogenesis, and that adult mesenchymal stem cells (MSCs) respond similarly as TPCs to embryonic developmental cues (Brown et al., 2014; Brown et al., 2015).

In earlier work, we demonstrated the ability to fabricate structurally uniform 3D alginate gels with uniform cell distribution and controllable mechanical properties as a function of Ca^{2+} concentration (i.e. crosslink density) and polymer concentration (Kuo and Ma, 2001). These alginate gels, favored for their highly controllable bulk-level mechanical properties, are now commonly utilized for tissue engineering (Jang et al., 2014; Korecki et al., 2009; Nunamaker et al., 2011). Here, we characterized the ability to control the cell length-scale mechanical properties of these gels, and to mimic the cell length-scale elastic moduli of embryonic tendon.

We hypothesized that TPCs are responsive to the cell length-scale mechanical properties of developing embryonic tendon. We engineered 3D alginate gel scaffolds with chick

embryonic tendon cell length-scale elastic moduli, and investigated the effects of these gels on chick embryo TPCs. The nano- and microscale elastic moduli of embryonic tendon were successfully achieved in ionically crosslinked alginate gels as a function of polymer concentration, crosslink density, arginyl-glycyl-aspartic acid (RGD)-peptide functionalization, and cell density. TPCs encapsulated within these alginate gels varied in cell morphology and tendon marker gene expression with differing initial nanoscale elastic moduli. Our results demonstrate scaffolds that recapitulate mechanical properties of embryonic tendon can regulate the behavior of tenogenically differentiating cells and potentially be remodeled during this process. These findings suggest developmentally inspired scaffolds may be useful for stem cell-based tendon tissue regeneration approaches.

2. Materials and Methods

2.1. Reagents

Unless otherwise stated, all reagents were from Sigma-Aldrich Co. (St. Louis, MO).

2.2. Primary TPC isolation

All animal procedures received approval from the Institutional Animal Care and Use Committee at Tufts University. Fertilized white leghorn chick embryos (UConn Poultry Farm, Storrs, CT) were cultured in a humidified rocking incubator at 37.5°C and sacrificed at Hamburger-Hamilton (HH) (Hamburger and Hamilton, 1951) stages 37 and 40. Calcaneus tendons were dissected from both limbs of ten HH 37 and six HH 40 chick embryos, and pooled for each stage. Tendons were digested in collagenase type II (1 mg/mL; Gibco, Grand Island, NY) with shaking at 200 RPM and 37°C, and then quenched with complete medium (CM) consisting of Dulbecco's Modified Eagle Medium (DMEM; Life Technologies), 10% fetal bovine serum (FBS; Atlanta Biologicals, Lawrenceville, GA), and 100 U/mL penicillin and 100 μg/mL streptomycin. The digested suspension was filtered through a 40-μm cell strainer. TPCs were expanded and used at passage 1–2.

2.3. Alginate functionalization

Purified low viscosity, high guluronate (60–70%) content alginate was obtained from FMC Biopolymer (Sandvika, Norway). The same lot of alginate was used for all experiments. We functionalized alginate with RGD peptides based on the protocol kindly provided by Dr. David Mooney (Drury et al., 2005; Rowley et al., 1999; Schiele et al., 2015). Alginate was suspended at 1% (w/v) in 0.3 M 4-morpholineethanesulfonic acid (MES) and 0.1 M NaCl, adjusted to pH 6.5 with NaOH, and functionalized with GGGGRGDSP peptides (Peptides International, Louisville, KY) using carbodiimide coupling. *N*-hydroxysulfosuccinimide (NHS), *N*-(3-Dimethylaminopropyl)-*N*′-ethylcarbodiimide hydrochloride (EDC), and RGD peptides were dissolved sequentially in mass ratios of 0.82, 1.64, and 0.03 relative to alginate, respectively. This reaction proceeded for 20 h at 22°C with stirring until termination by addition of hydroxylamine hydrochloride (HA) at a 0.043 mass ratio relative to alginate. Alginate solutions were dialyzed (3500 Da cut-off) for 72 h in distilled water, treated with activated charcoal, passed through a 0.2-μm filter, lyophilized, and re-suspended at 5% (w/v) in Hanks' Balanced Salt Solution without Ca^{2+} or Mg^{2+} (HBSS; Life Technologies, Grand Island, NY) to produce RGD-functionalized alginate (RGD-alg). This

process was replicated for “non-functionalized” alginate, which we designated as control (CTRL-alg), except that NHS, EDC, RGD, and HA were not included.

2.4. Fabrication of gels and culture of encapsulated TPCs

We fabricated alginate gels as previously described (Korecki et al., 2009; Kuo and Ma, 2001, 2008; Schiele et al., 2015). Briefly, alginate was mixed with $CaCO_3$ in HBSS to yield between a 1.5 to 4X Ca content, where “X Ca content” represents a molar ratio between added $CaCO_3$ and COOH groups on the alginate (Table 1) (Kuo and Ma, 2001). Trypsinized HH 40 TPCs were re-suspended in HBSS to yield either a final cell density of 1×10^6 (1 M/mL) or 10×10^6 cells/mL (10 M/mL). A fresh 21.4% (w/v) D-glucono-δ-lactone (GDL) solution in HBSS was then added in a 1:2 molar ratio of $CaCO_3$ to GDL. Final alginate concentrations were 1.5% or 3% (w/v). A 40-μL volume of alginate-cell solution was pipetted into custom 6-mm diameter polydimethylsiloxane molds (Dow Corning) and allowed to crosslink for 2 h at 37°C. RGD-alg gels and CTRL-alg gels encapsulating TPCs were transferred into 24-well plates and cultured at 37°C in CM, which was replaced every 48 h.

2.5. FV-AFM testing of gels

After 48 h of culture, gels were immersed in HBSS and immediately mechanically tested with FV-AFM, as we previously described for embryonic chick tendons and agarose gels (Marturano et al., 2013). Cantilevers with 0.06 N/m spring constants (Bruker, Camarillo, CA) and either 20 nm or 5 μm tip radius were employed for nano- and microscale measurements, respectively. Indentation force curves were measured over 10×10 μm^2 areas, with 256 indentations per area, at two different locations near the gel center. The linear regions of force curves were converted to elastic moduli using an empirically derived calibration curve developed with agarose gel standards, as previously described (Marturano et al., 2013). In previous work, we derived moduli of embryonic tendon from AFM measurements using either agarose gel standards or Hertzian theory calculations, and found that the two methods yielded similar values of embryonic tendon modulus over the entire range of development (Marturano et al., 2013). Three different gels were tested for each experimental condition.

2.6. Quantitative polymerase chain reaction (qPCR)

RGD-alg gels encapsulating 10 M/mL HH 37 TPCs were homogenized in TRIzol LS (Invitrogen) after 7 days of culture. Total RNA was extracted and quantified using spectrophotometry (Nanodrop ND-2000, Thermo Scientific, Wilmington, DE), and reverse-transcribed into cDNA using the Superscript III First-Strand Synthesis System (Invitrogen). QPCR was performed with Brilliant II SYBR Green qPCR Master Mix (Applied Biosystems, Foster City, CA) and the MX3000p qPCR System (Agilent Technologies, Santa Clara, CA). Chick-specific primer pairs were designed for tendon marker (scleraxis, tenomodulin, Col I, III, and XII) and housekeeping (18S) genes (Table 2). The $2^{-\Delta\Delta CT}$ method was used to calculate relative changes in gene expression. The data are presented as the fold change in target gene expression normalized to the housekeeping gene (18S), relative to HH 37 TPCs cultured in RGD-alg gels with an elastic modulus of 3.4 kPa. QPCR

was performed on HH 37 TPCs encapsulated in six RGD-alg gels for each elastic modulus condition.

2.7. Statistical analysis

All data are shown as mean ± standard deviation. To determine the statistical significance, Student's t-test or one-way ANOVA with Tukey's post-hoc test were performed using $p < 0.05$. All statistical calculations were performed with Graphpad (GraphPad Software Inc., San Diego, CA).

3. Results

3.1. Characterization of gel elastic modulus as a function of crosslink density and alginate concentration

FV-AFM was used to measure the elastic moduli of CTRL-alg gels encapsulating 1 M/mL HH 40 TPCs after 48 h of culture. Gels were tested as a function of crosslink density (Ca content) and alginate concentration. For gels of 1.5% (w/v) alginate, nanoscale elastic modulus ranged from 2.4 kPa to 6.0 kPa with significant differences ($p < 0.05$) between crosslink densities 1.5, 2, 3 and 4X Ca (Fig. 1A). Microscale elastic moduli ranged from 2.4 to 10 kPa, with significant differences ($p < 0.05$) between all crosslink densities except 1.5X and 2X Ca (Fig. 1B). The same trend was observed in 3% (w/v) alginate gels, with nanoscale elastic modulus increasing from 8 to 21 kPa with significant differences ($p < 0.05$) between all crosslink densities except 1.5X and 2X Ca (Fig. 1C). Microscale elastic modulus increased from 28 to 146 kPa, with significant differences ($p < 0.05$) detected between all crosslink densities except 3X and 4X Ca (Fig. 1D). When compared as a function of polymer concentration, elastic moduli were significantly higher ($p < 0.01$) in gels with 3% (w/v) alginate compared to 1.5% (w/v) alginate at all crosslink densities for both nanoscale (Fig. 1E) and microscale (Fig. 1F) measurements.

3.2 Effect of RGD-functionalization and cell density on gel elastic modulus and TPC morphology

Taking advantage of its "blank slate" nature, we functionalized alginate to present RGD to facilitate cell binding. FV-AFM was used to measure the elastic moduli of 1.5% (w/v) CTRL-alg and RGD-alg gels with 2X Ca content as a function of cell density (0, 1 or 10 M/mL HH 40 TPCs) after 48 h of culture. At a cell density of 0 M/mL (no cells), the elastic moduli of CTRL-alg gels were 5.2-fold greater than that of RGD-alg gels ($p = 0.0003$; Fig. 2A). At a cell density of 1 and 10 M/mL, the elastic moduli of RGD-alg gels were similar to that of CTRL-alg gels ($p = 0.33$ and 0.45 respectively; Fig. 2A). In CTRL-alg gels, TPCs appeared rounded, whereas TPCs in RGD-alg gels showed a spread, fibroblastic-like morphology, as seen in brightfield images (Fig. 2B). For each condition, there were no statistical differences in elastic modulus of gels containing 1 vs. 10 M/mL TPCs.

3.3 Gels possess embryonic tendon elastic moduli of different developmental stages

After we established the ability to control cell length-scale elastic moduli of alginate gels, we selected gels with elastic moduli of early-to-late embryonic tendons to examine their effects on TPCs. Based on our data (Fig. 1 and 2), nano- and microscale elastic moduli of

embryonic tendons at different developmental stages could be achieved with 3% (w/v) alg gels seeded with 1 M/mL TPCs and crosslinked from 1.5 to 4X Ca content (Fig. 3). At the microscale, alginate concentrations below 3% (w/v) will produce gels with moduli as low as HH 28 tendon. However, we chose to focus on the effects of nanoscale moduli on TPC responses because integrins that mediate cell-matrix interactions are nanoscale in dimension (Changede et al., 2015; Nermut et al., 1988).

3.4. Effect of RGD-alg gel elastic moduli on TPC morphology

To examine the effect of embryonic tendon nanoscale moduli on TPC morphology, 10 M/mL HH 37 TPCs were cultured for 7 days in RGD-alg gels. The gel elastic moduli ranged from 3.4 to 20.1 kPa, representative of early (< HH 28) to late stage (HH 43) embryonic tendons. Some TPCs appeared to spread in RGD-alg gels of 3.4 kPa by day 1, and by day 5 in 6.0 kPa RGD-alg gels (Fig. 4). In both 3.4 and 6.0 kPa RGD-alg gels, TPCs appeared to also establish cell-cell contacts by days 5 and 7. In contrast, TPCs retained a rounded morphology for all 7 days when cultured in RGD-alg gels fabricated with elastic moduli of 10.8 and 20.1 kPa, representing that of HH 30 to 43 embryonic tendons, respectively (Fig. 4).

3.5. Effect of RGD-alg gel elastic moduli on TPC gene expression

To evaluate the effects of different embryonic tendon nanoscale moduli on TPC gene expression, 10 M/mL HH 37 TPCs were cultured in RGD-alg gels for 7 days. The gels were fabricated with an elastic moduli ranging from 3.4 to 20.1 kPa to represent early (< HH 28) to late stage (HH 43) embryonic tendons. At 7 days, gene expression levels of Scleraxis and Col XII were significantly higher in TPCs in RGD-alg gels of 20.1 kPa, compared to TPCs in lower elastic modulus gels ($p < 0.05$; Fig. 5A and E). Tenomodulin expression appeared to be positively correlated with gel elastic modulus, but the differences in transcript levels between elastic moduli were not significant ($p > 0.05$; Fig. 5B). In contrast, Col I expression levels were significantly lower in RGD-alg gels of 10.8 and 20.1 kPa, compared to gels of 3.4 and 6.0 kPa ($p < 0.05$; Fig. 5C). Col III levels did not change with elastic modulus ($p > 0.05$; Fig. 5D).

4. Discussion

With the long-term goal of designing scaffolds to mechanoregulate tenogenic differentiation of stem cells for tissue engineering, we aimed to understand the effects of embryonic tendon mechanical properties on TPCs. TPCs isolated from embryonic tendon were selected as a model of tenogenically differentiating cells, whose behavior we have shown adult MSCs will mimic when cultured in tenogenic conditions (Brown et al., 2014; Brown et al., 2015). In this study, we developed an *in vitro* 3D culture system with which to investigate the influence of cell length-scale elastic modulus on TPC behavior, in isolation of the myriad of confounding factors *in vivo*. We established the ability to control nano- and microscale elastic moduli of alginate gels, and then demonstrated scaffolds that initially present with cell length-scale moduli of embryonic tendon can influence tenogenically differentiating cell morphology and gene expression. Our findings suggest embryonically inspired scaffolds could effectively guide stem cell tenogenesis in tendon engineering.

Both nano- and microscale elastic moduli of the alginate gels increased as a function of crosslink density (Ca^{2+} content) and polymer concentration (Fig. 1), agreeing with previous characterizations of alginate gel elastic modulus measured by bulk compression testing (Kuo and Ma, 2001). We attributed elastic modulus increases to a greater number of inter-chain crosslinks and polymer molecule entanglements. Similar to previous FV-AFM measurements of embryonic tendon elastic modulus (Marturano et al., 2013), the alginate gels had larger microscale elastic moduli than nanoscale elastic moduli. The microscale tip (5 μm radius) likely encountered resistance from a network of crosslinked and entangled polymer molecules, whereas the nanoscale tip (20 nm radius) may have detected individual molecules, as previously suggested in other tissue model systems (Loparic et al., 2010).

To facilitate cell adhesion within the gels, we functionalized the alginate with RGD, a common cell adhesion site found in fibronectin in developing tendons (Kuo et al., 2008). During functionalization, RGD peptides are covalently bound to the same carboxyl groups that divalent calcium ions crosslink between adjacent alginate chains during gelation. In the absence of cells, RGD functionalization reduced the microscale elastic modulus of the alginate gels, compared to non-functionalized (CTRL) alginate gels (Fig. 2A). However, encapsulation of 1 and 10 M/mL TPCs within the RGD-alg gels returned elastic modulus to the level of CTRL-alg gels (Fig. 2A). These observations were consistent at both the nano- and microscales, with no significant differences between CTRL-alg and RGD-alg gels seeded with 1 M/mL TPCs (Fig. 3A, B). Fibroblastic cell extensions in RGD-alg gels were suggestive of interactions between cells and the functionalized alginate, whereas no cell extensions were observed in CTRL-alg gels (Fig. 2B). Taken together, we attribute the increase in RGD-alg gel elastic modulus to crosslinks formed by the TPCs binding to RGD peptides on adjacent alginate chains. Similar phenomena for bulk scale mechanical properties of alginate gels have been suggested (Drury et al., 2005; Lee et al., 2003).

Cells interact with their physical environment via integrins. Considering integrins are nanoscale in dimension (Changede et al., 2015; Chen and Singer, 1982; Erb et al., 1997; Franz and Muller, 2005; Kanchanawong et al., 2010), we examined TPC responses to different nanoscale elastic moduli. RGD-alg gels differentially regulated tendon marker expression as a function of embryonic stage-specific nanoscale modulus after 7 days of culture. Scleraxis, an early stage marker for tendon progenitors during development (Murchison et al., 2007; Schweitzer et al., 2001), was expressed at significantly higher levels in RGD-alg gels with higher moduli, and at lower levels in RGD-alg gels with lower moduli (Fig. 5A). This was interesting, as Scleraxis levels during embryonic tendon development do not vary significantly (Brown et al., 2014; Brown et al., 2015; Havis et al., 2014). Col XII, which has been implicated in regulation of collagen fibrillogenesis (Zhang et al., 2003; Zhang et al., 2005), responded similarly as Scleraxis (Fig. 5E). In contrast, Col I, the primary component of adult tendon, was expressed at greater levels at lower elastic moduli (Fig. 5C). Both Tenomodulin (late stage tendon marker (Shukunami et al., 2006)) and Col III were not regulated by elastic modulus (Fig. 5B, D), perhaps reflecting the immature tenogenic stage of the HH 37 TPCs. At early developmental stages, TPCs may not yet be producing Col III, as Col III is thought to regulate Col I fibril diameter during relatively later stages of matrix synthesis and growth in embryonic tendon development (Birk and Mayne, 1997). We recently found that embryonic tendon elastic modulus and collagen content both

increase non-linearly throughout development, and that elastic modulus correlates with collagen crosslinker hydroxylysyl pyridinoline (HP) levels (Marturano et al., 2013; Marturano et al., 2014). Perhaps gels of lower elastic moduli, representative of earlier stage embryonic tendons, upregulated Col I expression in HH 37 TPCs to promote matrix production. Gels with higher elastic moduli could represent later stage embryonic tendons with higher collagen levels and HP crosslink density, signaling to cells that Col XII is needed to additionally regulate Col I fibrillogenesis.

Cell morphology varied with elastic modulus of RGD-alg gels. After 7 days of culture, the TPCs exhibited a fibroblastic morphology in RGD-alg gels of lower moduli (3.4 and 6 kPa), but maintained a rounded shape in RGD-alg gels of higher moduli (10.8 and 20.1 kPa) (Fig. 4). Others reported similar trends in morphology of adult MSCs in 3D, with greater cell spreading in softer gels and more cell rounding in stiffer gels (Maia et al., 2014). In contrast, the spread area of MSCs in monolayer culture is typically greater on stiffer substrates (Engler et al., 2006; Guvendiren and Burdick, 2012). In monolayer culture, cells interact with a substrate on one side and have no physical constraints otherwise, whereas cells are surrounding by matrix on all sides in a 3D scaffold. It has been proposed that cells maintain a rounded morphology in 3D when they cannot locally distort or remodel a structurally rigid and non-degradable matrix (Kuo and Smith, 2014; Maia et al., 2014). Here, the polymer networks at 10.8 and 20.1 kPa may have been too rigid to be deformed by the TPCs.

Cell morphology varied with crosslink density, and thus it is likely that complex interactions between elastic modulus and cell shape influenced crosslink density-specific changes in tendon marker expression. One study showed that increased RGD density leads to enhanced focal adhesion formation and alters MSC fate decisions (Trappmann et al., 2012), whereas others have reported substrate stiffness influences MSC differentiation independent of RGD density (Wen et al., 2014). Studies also suggest osteogenic and adipogenic MSC fate can be guided independently by scaffold modulus and cell morphology (Huebsch et al., 2010; Khetan et al., 2013). Additionally, hydrogel stress relaxation rate can influence cell spreading and differentiation independently of the hydrogel's initial elastic modulus and adhesion ligand density (Chaudhuri et al., 2016). We maintained constant alginate-to-RGD concentration ratios so that initial RGD concentrations did not vary with crosslink density. During culture, TPCs likely exerted cell traction and compacted local regions within lower crosslink density gels, effectively increasing local RGD density and modulus. Taken together, because TPC-matrix interactions are likely continuously altering the microenvironment, it is challenging to attribute TPC behavior to a particular scaffold parameter after 7 days of culture. On the other hand, because dynamic cell-matrix interactions are common in tissue remodeling, a critical aspect of development, one pragmatic approach is to design a scaffold that provides critical initial cues that trigger tenogenic cell behaviors, and that can also be remodeled by the TPCs in the formation of new tendon.

One concern is that adjusting calcium concentration to change crosslink density will trigger undesirable cell behaviors. In our formulations there were more alginate binding sites than calcium ions (Table 1), reducing the likelihood of free calcium ions in the system. Additionally, we used a controlled gelation method in which calcium ions are slowly

solubilized from $CaCO_3$ (Kuo and Ma, 2001) Considering calcium ion binding to alginate is uncontrollably rapid, the slow release of calcium ions from $CaCO_3$ helps to ensure rapid binding of calcium ions to carboxyl sites on alginate rather than being freely available at high enough concentrations that influence cell functions. Another consideration is whether increasing crosslinking density affects diffusivity of the gels. Given that TPC viability appeared unaffected and because we previously showed diffusion of proteins as large as bovine serum albumin through alginate gels is not inhibited at higher crosslink densities (Kuo and Ma, 2000), nutrient-waste exchange was likely not significantly compromised.

In summary, we showed that alginate gels can be fabricated with cell length-scale elastic moduli of embryonic tendons at distinct developmental stages, and that embryonic TPCs behave differently in 3D gels of different initial elastic moduli. Changes in cell morphology at the lower nanoscale elastic moduli representative of earlier stage embryonic tendons suggest TPCs were altering their local microenvironments during culture, as would also be expected during tissue development *in vivo*. Embryonic tendon mechanical properties change during development (Marturano et al., 2013), presumably due to cells continually remodeling their microenvironments while building new tissue. Thus, the initial extracellular matrix cues provided to stem cells are critically important in promoting differentiation and neotissue formation and are expected to change during this process.

Specific cell-matrix interactions that promote desirable tenogenic outcomes will be the subject of future study. We previously demonstrated embryonic TPCs are an excellent model of tenogenically differentiating cells, and that MSCs respond tenogenically to microenvironments that are tenogenic for TPCs (Brown et al., 2014; Brown et al., 2015). Future studies to compare MSC and TPC behavior in these alginate hydrogel scaffolds with embryonic vs. adult mechanical properties will advance scaffold-based approaches to regulate stem cell tenogenesis. Our findings lay the groundwork to investigate embryonically inspired scaffolds as effective tools for tendon tissue engineering with stem cells.

Acknowledgments

We gratefully acknowledge funding support by the NIH Training in Education and Critical Research Skills (K12GM074869) postdoctoral program (to N.R.S.), Research Grant 5-FY11-153 from the March of Dimes Foundation (to C.K.K.) and Award Number R03AR061036 from the NIH (to C.K.K.).

References

AAOS. United States Bone and Joint Decade: The Burden of Musculoskeletal Diseases in the United States. American Academy of Orthopaedic Surgeons; Rosemont, IL: 2008.

Birk DE, Mayne R. Localization of collagen types I, III and V during tendon development. Changes in collagen types I and III are correlated with changes in fibril diameter. European journal of cell biology. 1997; 72:352–361. [PubMed: 9127735]

Brown JP, Finley VG, Kuo CK. Embryonic mechanical and soluble cues regulate tendon progenitor cell gene expression as a function of developmental stage and anatomical origin. J Biomech. 2014; 47:214–222. [PubMed: 24231248]

Brown JP, Galassi TV, Stoppato M, Schiele NR, Kuo CK. Comparative analysis of mesenchymal stem cell and embryonic tendon progenitor cell response to embryonic tendon biochemical and mechanical factors. Stem cell research & therapy. 2015; 6:89. [PubMed: 25956970]

Butler DL, Juncosa N, Dressler MR. Functional efficacy of tendon repair processes. Annual review of biomedical engineering. 2004; 6:303–329.

Chainani A, Hippensteel KJ, Kishan A, Garrigues NW, Ruch DS, Guilak F, Little D. Multilayered electrospun scaffolds for tendon tissue engineering. Tissue Eng Part A. 2013; 19:2594–2604. [PubMed: 23808760]

Changede R, Xu XC, Margadant F, Sheetz MP. Nascent Integrin Adhesions Form on All Matrix Rigidities after Integrin Activation. Developmental Cell. 2015:35.

Chaudhuri O, Gu L, Klumpers D, Darnell M, Bencherif SA, Weaver JC, Huebsch N, Lee HP, Lippens E, Duda GN, Mooney DJ. Hydrogels with tunable stress relaxation regulate stem cell fate and activity. Nature materials. 2016; 15:326–334. [PubMed: 26618884]

Chen WT, Singer SJ. Immunoelectron Microscopic Studies of the Sites of Cell-Substratum and Cell-Cell Contacts in Cultured Fibroblasts. J Cell Biol. 1982; 95:205–222. [PubMed: 6815205]

Chokalingam K, Juncosa-Melvin N, Hunter SA, Gooch C, Frede C, Florert J, Bradica G, Wenstrup R, Butler DL. Tensile stimulation of murine stem cell-collagen sponge constructs increases collagen type I gene expression and linear stiffness. Tissue Eng Part A. 2009; 15:2561–2570. [PubMed: 19191514]

Drury JL, Boontheekul T, Mooney DJ. Cellular cross-linking of peptide modified hydrogels. J Biomech Eng. 2005; 127:220–228. [PubMed: 15971699]

Engler AJ, Sen S, Sweeney HL, Discher DE. Matrix Elasticity Directs Stem Cell Lineage Specification. Cell. 2006; 126:677–689. [PubMed: 16923388]

Erb EM, Tangemann K, Bohrmann B, Muller B, Engel J. Integrin alpha IIb beta 3 reconstituted into lipid bilayers is nonclustered in its activated state but clusters after fibrinogen binding. Biochemistry. 1997; 36:7395–7402. [PubMed: 9200686]

Franz CM, Muller DJ. Analyzing focal adhesion structure by atomic force microscopy. J Cell Sci. 2005; 118:5315–5323. [PubMed: 16263758]

Guvendiren M, Burdick JA. Stiffening hydrogels to probe short- and long-term cellular responses to dynamic mechanics. Nat Commun. 2012; 3:792. [PubMed: 22531177]

Hamburger V, Hamilton HL. A Series of Normal Stages in the Development of the Chick Embryo. Journal of Morphology. 1951; 88:49–92. [PubMed: 24539719]

Havis E, Bonnin MA, Olivera-Martinez I, Nazaret N, Ruggiu M, Weibel J, Durand C, Guerquin MJ, Bonod-Bidaud C, Ruggiero F, Schweitzer R, Duprez D. Transcriptomic analysis of mouse limb tendon cells during development. Development. 2014; 141:3683–3696. [PubMed: 25249460]

Huebsch N, Arany PR, Mao AS, Shvartsman D, Ali OA, Bencherif SA, Rivera-Feliciano J, Mooney DJ. Harnessing traction-mediated manipulation of the cell/matrix interface to control stem-cell fate. Nature materials. 2010; 9:518–526. [PubMed: 20418863]

Jang J, Seol YJ, Kim HJ, Kundu J, Kim SW, Cho DW. Effects of alginate hydrogel cross-linking density on mechanical and biological behaviors for tissue engineering. J Mech Behav Biomed Mater. 2014; 37:69–77. [PubMed: 24880568]

Kanchanawong P, Shtengel G, Pasapera AM, Ramko EB, Davidson MW, Hess HF, Waterman CM. Nanoscale architecture of integrin-based cell adhesions. Nature. 2010; 468:580–U262. [PubMed: 21107430]

Khetan S, Guvendiren M, Legant WR, Cohen DM, Chen CS, Burdick JA. Degradation-mediated cellular traction directs stem cell fate in covalently crosslinked three-dimensional hydrogels. Nature materials. 2013; 12:458–465. [PubMed: 23524375]

Korecki CL, Kuo CK, Tuan RS, Iatridis JC. Intervertebral disc cell response to dynamic compression is age and frequency dependent. J Orthop Res. 2009; 27:800–806. [PubMed: 19058142]

Kuo CK, Ma PX. Controlling Diffusion of Solutes Through Ionically Crosslinked Alginate Hydrogels Designed for Tissue Engineering. MRS Proceedings. 2000:662.

Kuo CK, Ma PX. Ionically crosslinked alginate hydrogels as scaffolds for tissue engineering: part 1. Structure, gelation rate and mechanical properties. Biomaterials. 2001; 22:511–521. [PubMed: 11219714]

Kuo CK, Ma PX. Maintaining dimensions and mechanical properties of ionically crosslinked alginate hydrogel scaffolds in vitro. J Biomed Mater Res A. 2008; 84:899–907. [PubMed: 17647237]

Kuo CK, Marturano JE, Tuan RS. Novel strategies in tendon and ligament tissue engineering: Advanced biomaterials and regeneration motifs. Sports Med Arthrosc Rehabil Ther Technol. 2010; 2:20. [PubMed: 20727171]

Kuo CK, Petersen BC, Tuan RS. Spatiotemporal protein distribution of TGF-betas, their receptors, and extracellular matrix molecules during embryonic tendon development. Dev Dyn. 2008; 237:1477–1489. [PubMed: 18425852]

Kuo CK, Smith ML. Biomaterial design motivated by characterization of natural extracellular matrices. MRS Bull. 2014; 39:18–24.

Kuo CK, Tuan RS. Mechanoactive tenogenic differentiation of human mesenchymal stem cells. Tissue Eng Part A. 2008; 14:1615–1627. [PubMed: 18759661]

Lantto I, Heikkinen J, Flinkkila T, Ohtonen P, Leppilahti J. Epidemiology of Achilles tendon ruptures: increasing incidence over a 33-year period. Scand J Med Sci Sports. 2015; 25:e133–138. [PubMed: 24862178]

Lee KY, Kong HJ, Larson RG, Mooney DJ. Hydrogel formation via cell crosslinking. Adv Mater. 2003; 15:1828–1832.

Lin TW, Cardenas L, Soslowsky LJ. Biomechanics of tendon injury and repair. J Biomech. 2004; 37:865–877. [PubMed: 15111074]

Loparic M, Wirz D, Daniels AU, Raiteri R, Vanlandingham MR, Guex G, Martin I, Aebi U, Stolz M. Micro- and nanomechanical analysis of articular cartilage by indentation-type atomic force microscopy: validation with a gel-microfiber composite. Biophysical Journal. 2010; 98:2731–2740. [PubMed: 20513418]

Maia FR, Fonseca KB, Rodrigues G, Granja PL, Barrias CC. Matrix-driven formation of mesenchymal stem cell-extracellular matrix microtissues on soft alginate hydrogels. Acta Biomater. 2014; 10:3197–3208. [PubMed: 24607421]

Marturano JE, Arena JD, Schiller ZA, Georgakoudi I, Kuo CK. Characterization of mechanical and biochemical properties of developing embryonic tendon. Proc Natl Acad Sci U S A. 2013; 110:6370–6375. [PubMed: 23576745]

Marturano JE, Xylas JF, Sridharan GV, Georgakoudi I, Kuo CK. Lysyl oxidase-mediated collagen crosslinks may be assessed as markers of functional properties of tendon tissue formation. Acta Biomater. 2014; 10:1370–1379. [PubMed: 24316363]

Murchison ND, Price BA, Conner DA, Keene DR, Olson EN, Tabin CJ, Schweitzer R. Regulation of tendon differentiation by scleraxis distinguishes force-transmitting tendons from muscle-anchoring tendons. Development. 2007; 134:2697–2708. [PubMed: 17567668]

Nermut MV, Green NM, Eason P, Yamada SS, Yamada KM. Electron microscopy and structural model of human fibronectin receptor. EMBO J. 1988; 7:4093–4099. [PubMed: 2977331]

Nirmalanandhan VS, Rao M, Shearn JT, Juncosa-Melvin N, Gooch C, Butler DL. Effect of scaffold material, construct length and mechanical stimulation on the in vitro stiffness of the engineered tendon construct. J Biomech. 2008; 41:822–828. [PubMed: 18164020]

Nunamaker EA, Otto KJ, Kipke DR. Investigation of the material properties of alginate for the development of hydrogel repair of dura mater. J Mech Behav Biomed Mater. 2011; 4:16–33. [PubMed: 21094477]

Qiu Y, Lei J, Koob TJ, Temenoff JS. Cyclic tension promotes fibroblastic differentiation of human MSCs cultured on collagen-fibre scaffolds. Journal of tissue engineering and regenerative medicine. 2014

Rowley JA, Madlambayan G, Mooney DJ. Alginate hydrogels as synthetic extracellular matrix materials. Biomaterials. 1999; 20:45–53. [PubMed: 9916770]

Schiele NR, Marturano JE, Kuo CK. Mechanical factors in embryonic tendon development: potential cues for stem cell tenogenesis. Curr Opin Biotechnol. 2013; 24:834–840. [PubMed: 23916867]

Schiele NR, von Flotow F, Tochka ZL, Hockaday LA, Marturano JE, Thibodeau JJ, Kuo CK. Actin cytoskeleton contributes to the elastic modulus of embryonic tendon during early development. J Orthop Res. 2015; 33:874–881. [PubMed: 25721681]

Schiller ZA, Schiele NR, Sims JK, Lee K, Kuo CK. Adipogenesis of adipose-derived stem cells may be regulated via the cytoskeleton at physiological oxygen levels in vitro. Stem cell research & therapy. 2013; 4:79. [PubMed: 23838354]

Schweitzer R, Chyung JH, Murtaugh LC, Brent AE, Rosen V, Olson EN, Lassar A, Tabin CJ. Analysis of the tendon cell fate using Scleraxis, a specific marker for tendons and ligaments. Development. 2001; 128:3855–3866. [PubMed: 11585810]

Shukunami C, Takimoto A, Oro M, Hiraki Y. Scleraxis positively regulates the expression of tenomodulin, a differentiation marker of tenocytes. Dev Biol. 2006; 298:234–247. [PubMed: 16876153]

Subramony SD, Dargis BR, Castillo M, Azeloglu EU, Tracey MS, Su A, Lu HH. The guidance of stem cell differentiation by substrate alignment and mechanical stimulation. Biomaterials. 2013; 34:1942–1953. [PubMed: 23245926]

Trappmann B, Gautrot JE, Connelly JT, Strange DG, Li Y, Oyen ML, Cohen Stuart MA, Boehm H, Li B, Vogel V, Spatz JP, Watt FM, Huck WT. Extracellular-matrix tethering regulates stem-cell fate. Nature materials. 2012; 11:642–649. [PubMed: 22635042]

Wen JH, Vincent LG, Fuhrmann A, Choi YS, Hribar KC, Taylor-Weiner H, Chen S, Engler AJ. Interplay of matrix stiffness and protein tethering in stem cell differentiation. Nature materials. 2014; 13:979–987. [PubMed: 25108614]

Xie J, Li X, Lipner J, Manning CN, Schwartz AG, Thomopoulos S, Xia Y. “Aligned-to-random” nanofiber scaffolds for mimicking the structure of the tendon-to-bone insertion site. Nanoscale. 2010; 2:923–926. [PubMed: 20648290]

Zhang G, Young BB, Birk DE. Differential expression of type XII collagen in developing chicken metatarsal tendons. J Anat. 2003; 202:411–420. [PubMed: 12739618]

Zhang G, Young BB, Ezura Y, Favata M, Soslowsky LJ, Chakravarti S, Birk DE. Development of tendon structure and function: regulation of collagen fibrillogenesis. J Musculoskelet Neuronal Interact. 2005; 5:5–21. [PubMed: 15788867]

Zhang X, Bogdanowicz D, Erisken C, Lee NM, Lu HH. Biomimetic scaffold design for functional and integrative tendon repair. J Shoulder Elbow Surg. 2012; 21:266–277. [PubMed: 22244070]

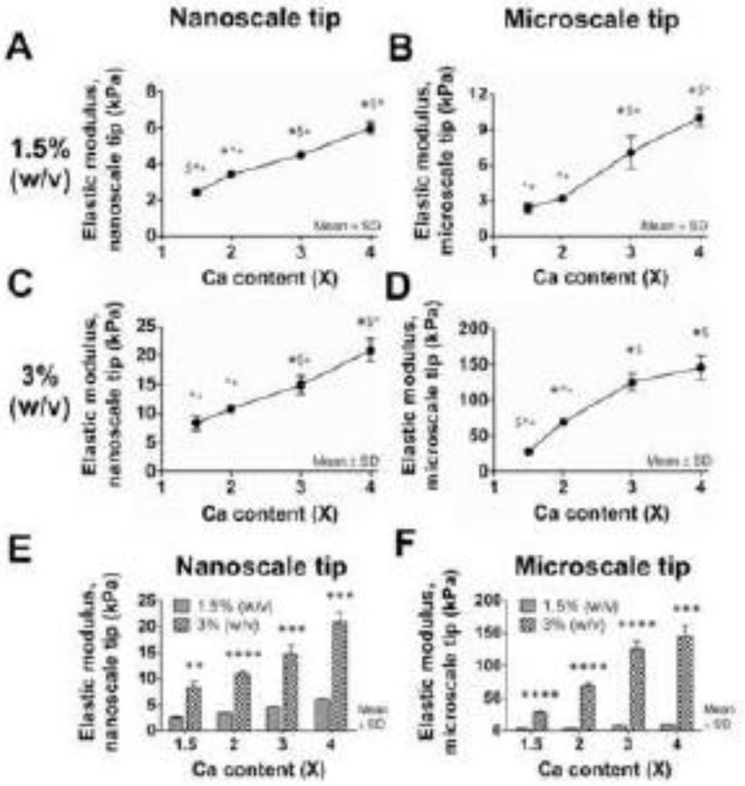

Fig. 1. Gel elastic modulus as a function of crosslink density and alginate concentration

The (**A, C**) nanoscale and (**B, D**) microscale elastic moduli of CTRL-alg gels seeded with 1 M/mL HH 40 TPCs were measured with FV-AFM after 48 h of culture. The elastic moduli of (**A, B**) 1.5 % (w/v) and (**C, D**) 3% (w/v) alginate gels increased with increasing calcium content. n = 3 gels per condition. Statistical significance between different calcium contents is denoted with symbols: * versus 1.5X; $ versus 2X: ^ versus 3X; + versus 4X, where *; $; ^; + denote $p < 0.05$. The (**E**) nanoscale and (**F**) microscale elastic moduli of 3% (w/v) alginate gels were significantly higher than the elastic moduli of 1.5% (w/v) alginate gels with the same calcium content. n = 3 gels per condition; * $p < 0.05$; ** $p < 0.01$; *** $p<0.001$; **** $p<0.0001$.

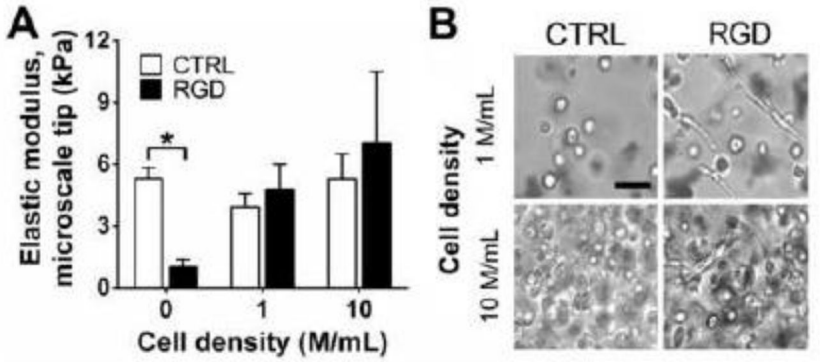

Fig. 2. Effect of RGD-functionalization and cell density on gel elastic modulus and TPC morphology

(**A**) Elastic moduli of 1.5% (w/v) alginate gels at 2X calcium content were measured with FV-AFM as a function of RGD functionalization and HH 40 TPC density after 48 h of culture. At a cell density of 0 M/mL, the elastic modulus of RGD-alg gels was significantly lower than CTRL-alg gels. The elastic moduli of CTRL- and RGD-alg gels seeded with 1 and 10 M/mL TPCs were not significantly different. n = 3 gels per condition; * $p < 0.05$. (**B**) Representative brightfield images of CTRL and RGD-alg gels seeded 1 and 10 M/mL TPCs after 48 h of culture. At both cell densities, TPCs exhibited round morphology in CTRL-alg gels, while TPCs exhibited spread morphology in RGD-alg gels. Bar = 50 μm.

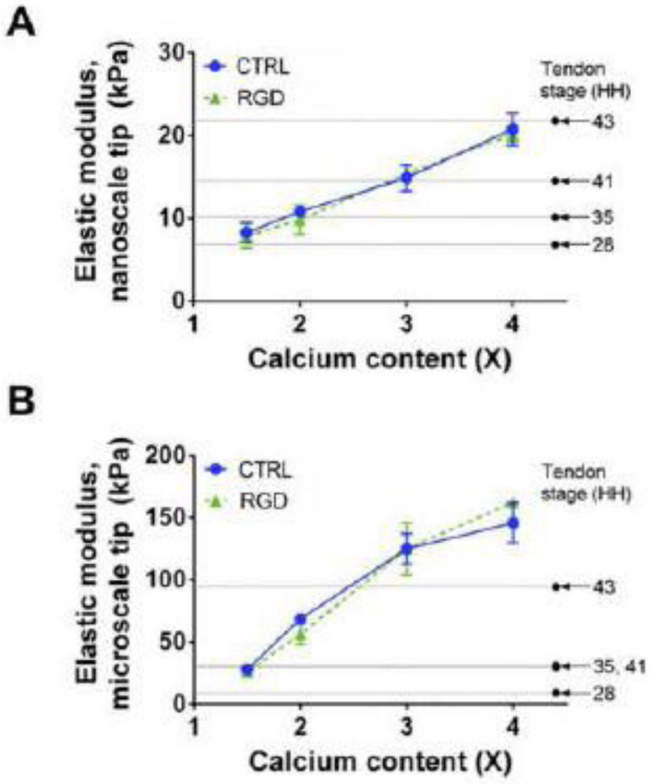

Fig. 3. Gels possess embryonic tendon elastic moduli of different developmental stages

Elastic moduli of 3% (w/v) alginate gels seeded with 1 M/mL HH 40 TPCs possess average elastic modulus of HH 28, 35, 41 and 43 embryonic chick tendons at the nanoscale (**A**) and the microscale (**B**), when crosslinked with 1.5 to 4X Ca. At both nano- and microscales there were no significant differences in the elastic moduli between CTRL- and RGD-alg gels at the same calcium content. n = 3 gels per condition. Mean elastic moduli of embryonic chick tendon from Marturano et al., 2013 (Marturano et al., 2013).

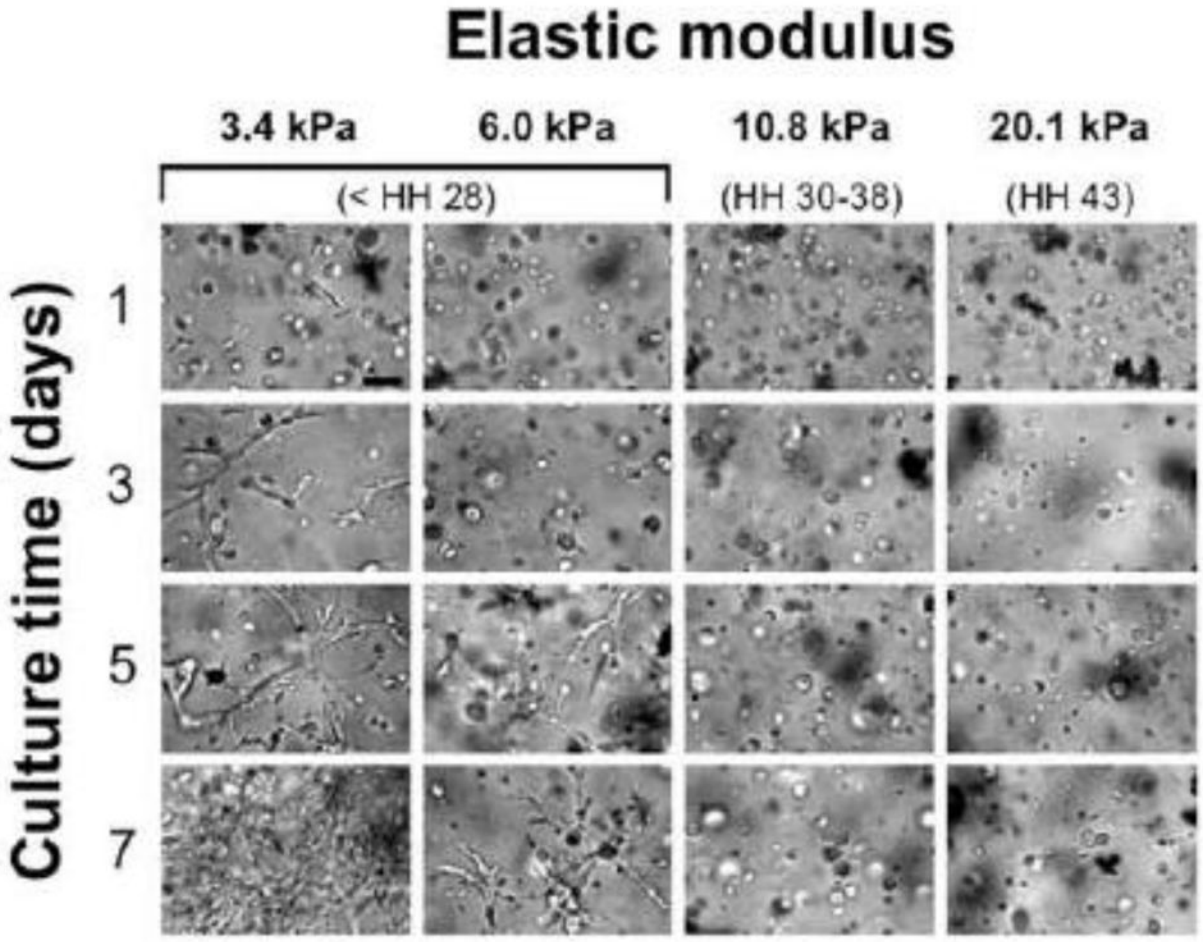

Fig. 4. Effect of RGD-alg gel elastic moduli on TPC morphology

Representative brightfield images of RGD-alg gels seeded with 10 M/mL HH 37 TPCs and cultured for 7 days. RGD-alg gels with nanoscale elastic moduli from 3.4 to 20.1 kPa represented embryonic tendon from < HH 28 to HH 43. Cell spreading was first observed after 1 day of culture in gels of 3.4 kPa and after 5 days in gels of 6.0 kPa. TPCs maintained rounded morphology in gels of 10.8 and 20.1 kPa. Bar = 50 μm.

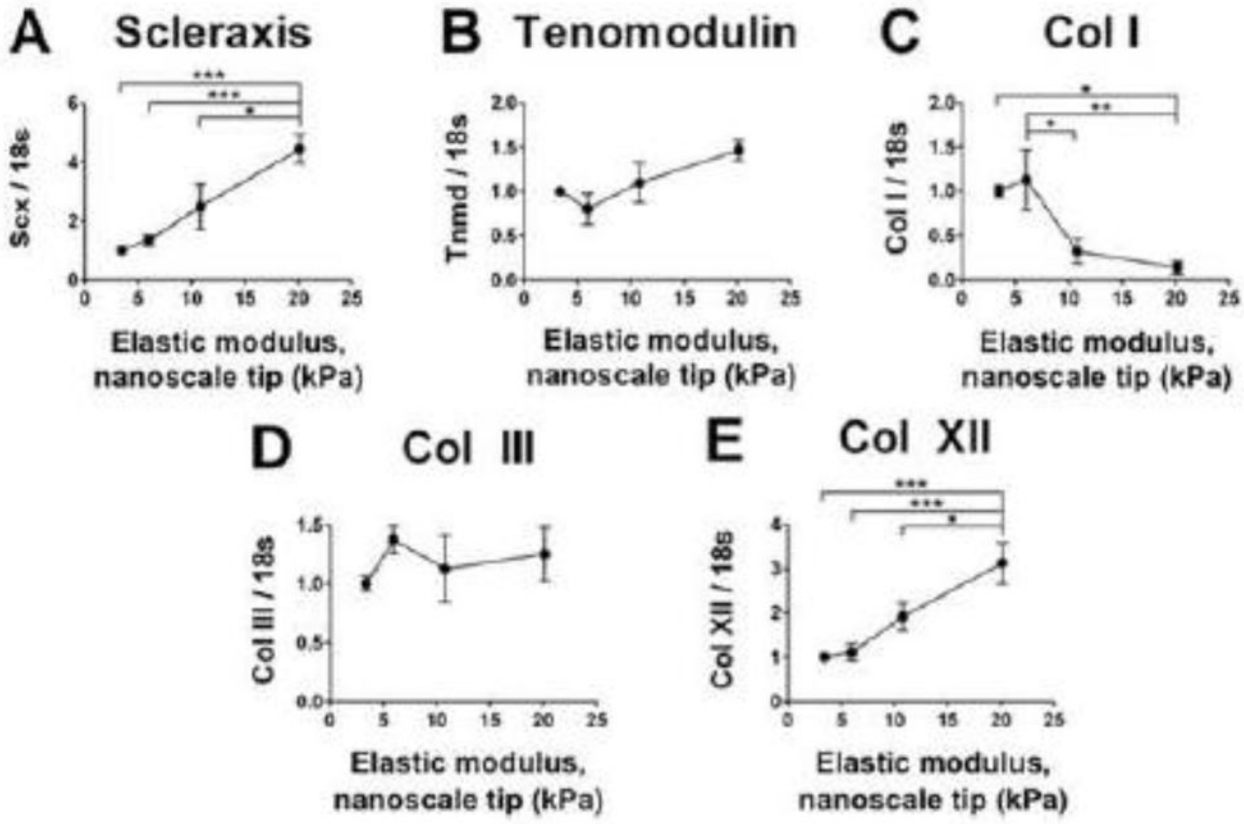

Fig. 5. Effect of RGD-alg gel elastic moduli on TPC gene expression

Tendon marker genes expressed by 10 M/mL HH 37 TPCs cultured in RGD-alg gels for 7 days. RGD-alg gels of nanoscale elastic moduli from 3.4 to 20.1 kPa represented embryonic tendon from < HH 28 to HH 43. Elastic modulus significantly influenced the expression of (**A**) scleraxis, (**C**) Col I, and (**E**) Col XII, but did not significantly influence expression of (**B**) tenomodulin or (**D**) Col III. n = 6 gels per condition; * $p < 0.05$; ** $p < 0.01$; *** $p < 0.001$.

Table 1

Ca content (X) and corresponding Ca-to-COOH molar ratio used in calculations for $CaCO_3$ and alginate.

Ca content (X)	Ca/COOH (mol/mol)
1.5X	0.27
2X	0.36
3X	0.54
4X	0.72

Table 2

Forward and reverse primer sequences designed for qPCR.

Gene	Accession No.	Forward sequence	Reverse sequence
18S	AF173612.1	CGGGGCCATGATTAAGAGGG	CTTTAGTTCGTCTTGCGCCG
Col I	NM_001079714.1	CCAGGACAACCTGGTGCTCGC	CAGCGCTGCCATCACTCCCA
Col III	NM_205380.2	TTCAGGAGCAAGGGGTCCACC	AGGGAAGCTACGCCACCACCA
Col XII	NM_205021.1	CCACATCAGCCACACCCACAA	CAGACGGACAGGCAAAGCCCT
Tenomodulin	NM_206985.2	CATGGTCTGGGTGCCTGGCG	TCCGGAGCTGCTATCGGGGT
Scleraxis	NM_204253.1	CGCGACAGGAAGACGGCGAT	CTGGCAGCGGGGTGAAGACG